View metadata, citation and similar papers at core.ac.uk

brought to you by CORE

provided by PolyU Institutional Repository

JOURNAL OF APPLIED PHYSICS VOLUME 95, NUMBER 7 1 APRIL 2004

X-ray photoemission spectroscopy of nonmetallic materials: Electronic structures of boron and B_xO_y

C. W. Ong and H. Huang
Department of Applied Physics, The Hong Kong Polytechnic University, Hung Hom, Kowloon, Hong Kong, China

B. Zheng and R. W. M. Kwok
Department of Chemistry, and Materials Science and Technology Research Centre, The Chinese University of Hong Kong, Shatin, N.T., Hong Kong, China

Y. Y. Hui and W. M. Lau[a]
Department of Physics, The Chinese University of Hong Kong, Shatin, N.T., Hong Kong, China

(Received 5 May 2003; accepted 7 January 2004)

Although an increasing volume of x-ray photoemission spectroscopic (XPS) data has been accumulated on boron and boron-rich compounds because of their unusual properties, including a unique three-center, two-electron bonding configuration, their common nonmetallic nature has been overlooked. Typically, the measured energy-state data are not clarified by surface Fermi level positions of these nonmetallic samples, which compromises the scientific contents of the data. In the present study, we revisited the XPS studies of sputter-cleaned β-rhombohedral boron (β_r-B), the oxidized surface of β_r-B, B_6O pellet, and polished B_2O_3, to illustrate the impact and resolution of this scientific issue. These samples were chosen because β_r-B is the most thermodynamically stable polytype of pure boron, B_2O_3 is its fully oxidized form, and B_6O is the best known superhard family member of boron-rich compounds. From our XPS measurements, including those from a sputter-cleaned gold as a metal reference, we deduced that our β_r-B had a surface Fermi level located at 0.7 ± 0.1 eV from its valence-band maximum (VBM) (referred as E_{FL}) and a binding energy for its B $1s$ core level at 187.2 eV from VBM ($E_{b,\mathrm{VBM}}$). The latter attribute, unlike typical XPS binding energy data that are referenced to a sample-dependent Fermi level ($E_{b,\mathrm{FL}}$), is immune from any uncertainties and variations arising from sample doping and surface charging. For bulk B_2O_3, we found an $E_{b,\mathrm{VBM}}$ for its B $1s$ core level at 190.5 eV and an $E_{b,\mathrm{FL}}$ at 193.6 eV. For our β_r-B subjected to a surface oxidation treatment, an overlayer structure of $\sim 1.2\,\mathrm{nm}\,B_2O_3/\sim 2\,\mathrm{nm}\,B_2O/B$ was found. By comparing the data from this sample and those from β_r-B and bulk B_2O_3, we infer that the oxide overlayer carried some negative fixed charge and this induced on the semiconducting β_r-B sample an upward surface band bending of $\sim$0.6 eV. As for our B_6O sample, we found an E_{FL} of $\sim$1.7 eV and two different chemical states having $E_{b,\mathrm{VBM}}$ of 185.4 and 187.2 eV, with the former belonging to boron with no oxygen neighbor and the latter to boron with an oxygen neighbor. The methodology in this work is universally applicable to all nonmetallic samples.
© *2004 American Institute of Physics.* [DOI: 10.1063/1.1651321]

I. INTRODUCTION

X-ray photoelectron spectroscopy (XPS) is a useful analytical tool for research on electronic structures for both metals and nonmetallic materials.[1,2] In a concise description, XPS gives binding energies of electrons in occupied states relative to the Fermi level (FL) of the materials (referred to as $E_{b,\mathrm{FL}}$). Normally, binding energy reflects the chemical state of the chemical element emitting the corresponding photoelectrons, and is sensitive to chemical changes such as oxidation or bonding with strongly electronegative/electropositive elements. However, for a nonmetallic material, the presence of impurities or charge-trapping defects with an amount much less than the detection limit of XPS, can also largely affect its FL position (E_{FL}). In such a case, $E_{b,\mathrm{FL}}$ becomes a variable dependent on the occupancies of the energy states of impurities and charge-trapping defects of the material, and such occupancies may also be affected by other extrinsic factors such as the presence of an overlayer of other materials or a sheet of surface charge. The following examples show how much these attributes can affect binding energy data in XPS.

- **Effect of E_{FL} due to the presence of impurity in a semiconductor**. Pure silicon has an E_{FL} at 0.54 eV and silicon with 1 ppm of boron has an E_{FL} at 0.14 eV. The binding energy difference is 0.40 eV.
- **Chemical state effect**. Metallic silicides are known to possess different and therefore characteristic binding energies.[1]
- **Band bending effect**. For a p-Si (doped with 1 ppm of boron) sample having an oxide overlayer of 5 nm, its

[a]Author to whom correspondence should be addressed; electronic mail: leol@phy.cuhk.edu.hk

Downloaded 07 Apr 2011 to 158.132.161.9. Redistribution subject to AIP license or copyright; see http://jap.aip.org/about/rights_and_permissions

E_{FL} should still be 0.14 eV if there is no trapped charge in the oxide and at the interface. If a sheet of positive unit charge is deposited on the surface of this sample to an amount of 7.3×10^{11} cm^2, the binding energy of the oxide will be increased by 0.97 eV and that of silicon will be increased by 0.80 eV. The changes are caused by surface band bending of the oxide and the semiconductor induced by the positive surface charge and its electrical potential. This set of band bending conditions is practically used in microelectronics for switching a typical *n*-channel metal-oxide–semiconductor field-effect transistor from off to on.

The present article uses a detailed analysis of boron and B_xO_y compounds as an example to further illustrate this concept and to show that although these interesting boron-containing materials[3–20] are known to be nonmetallic, previous XPS studies on them,[9,10,15–19] have not examined their E_{FL} values, the factors affecting these values, and the XPS data affected by the E_{FL} changes. Because of these deficiencies, some of the data are seemingly contradictory and the science is veiled. The objective is to show that with a set of simple and practical analysis guidelines, these deficiencies can be addressed adequately and a scientific picture of the bonding nature of these materials can be constructed.

Boron and B_xO_y compounds are interesting nonmetallic materials. Boron and many boron-rich compounds commonly possess extreme hardness, and intriguing solid-state structures constructed by a building block of twelve boron atoms in an icosahedron.[3,4] In each icosahedron, boron atoms are bound together tightly by rather unique three-center, two-electron bonds. These icosahedra are then typically connected by the normal two-center, two-electron bonds. For example, the α- and β-rhombohedral, and α- and β-tetragonal crystal forms of boron are all built this way. Among these, β-rhombohedral boron (referred as β_r-B in this article) is the most thermodynamically stable and widely available, and the α-rhombohedral boron is the hardest with a microhardness value of ~27 GPa (in comparison, the respective values for diamond and various tungsten carbide products are ~100 and ~15–20 GPa). In the context of the present work, we stress that boron is nonmetallic. For example, β_r-B is known to have a bandgap of ~1.6 eV, and a set of acceptor and donor states in the bandgap has also been identified by optical and luminescence studies.[5] It is expected that β_r-B, having different electron occupancies in these electronic structures, will have different physical and chemical behaviors.

Intuitively, one would infer that adding atoms with more valence electrons than boron into the boron lattice structures built by the electron-deficient B_{12} icosahedra may further strengthen the cohesiveness of the icosahedra, leading to interesting changes in both electrical and mechanical properties. Indeed, a variety of boron-rich compounds has already been discovered, with carbon, oxygen, nitrogen, and phosphorus as the most common additives.[3–6] Among them, the B_xO_y family is particularly versatile. Its most "mature" member is B_2O_3, in which boron is fully oxidized to an oxidation number of +3. The material is widely used in the production of glass and other ceramic products. At the low

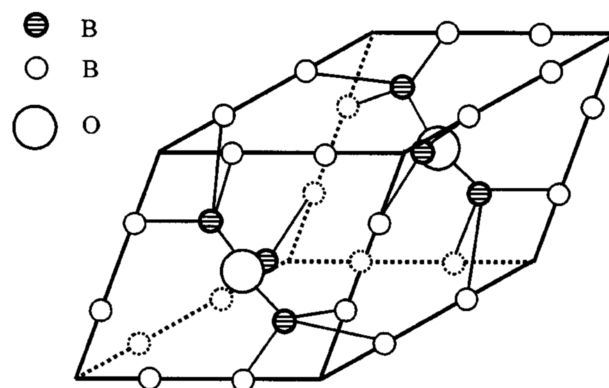

FIG. 1. Crystal unit cell and bonding configuration of B_6O.

end of the y/x spectrum, one finds $B_{22}O$, which was claimed to be hard enough to generate wear grooves on (111) diamond faces.[7] Although no further data on this particular compound have ever been seen, the presence of a superhard B_xO_y family has been convincingly substantiated by subsequent reports on the synthesis and characterization of family members[3] such as B_7O, B_6O, B_2O, etc. Among them, B_6O is the best known in both materials properties[3,7–14] and industrial applications.[13] For example, the most recent report[14] on this materials gives a high hardness of 45 GPa from a single-crystal grain of B_6O. It is also known[11,12] that B_6O is a semiconductor with a bandgap of about 2 eV. In addition, research on thin-film deposition of B_6O has also yielded some encouraging results.[20] Further development of the science and technology of these lightweight boron and boron compounds will require accurate analysis of materials identities and electronic structures of these materials.

For example, the scientific picture of B_6O is still evolving. Crystallographic studies[9,12] of B_6O have revealed structural information relevant to its high hardness and cohesive energy. As shown in Fig. 1, the unit cell of B_6O contains twelve boron atoms and two oxygen atoms, with all boron atoms belonging to B_{12} icosahedra surrounding the unit cell. Six of the boron atoms (the shaded ones in Fig. 1) have an oxygen atom as their neighbors. The unit cell shows 24 boron atoms (the small open circles in Fig. 1) having no neighboring oxygen, but each of them shared by four unit cells. Hence, in the traditional chemical state description, the unit cell of B_6O actual has a nominal composition of $B_{12}O_2$, with a total of six boron atoms having an oxidation number of zero (referred as the "B_3" group of elemental boron in the present work) and a total of six boron atoms having an oxidation number of $+\frac{1}{3}$ (suboxide). These suboxide atoms are equivalent to those of a hypothetical "B_3O" species and are thus referred as the B_3O group in the present work. Direct experimental verification of these two bonding configurations have indeed been accomplished by Moddeman *et al.*,[9] who demonstrated that B_6O really has two B 1*s* core-level peaks with almost equal intensity and a binding energy separation by about 1.6–1.7 eV. This early study and an XPS revisit[10] of B_6O, however, both missed the semiconductor nature of the material. In fact, such a deficiency is commonly found in XPS of boron, B_xO_y, and many other nonmetallic

Downloaded 07 Apr 2011 to 158.132.161.9. Redistribution subject to AIP license or copyright; see http://jap.aip.org/about/rights_and_permissions

materials. The present work aims to show that the deficiency can be eliminated easily during XPS analysis of nonmetallic materials, and a little caution can yield good scientific insights.

II. EXPERIMENTAL METHODS

A. Sample preparation

Polycrystalline β_r-B chips with a purity of 99.5% and sizes around 5 mm were supplied by Aldrich Chemical Company, Inc. A crystal chip was polished by using fine diamond paste, and then cleaned. Surface oxidation of the crystal was conducted with a tube furnace set at 700 °C for 5 min and a wet oxygen flow. For the B_6O preparation, we modified the synthesis procedures of Kayhan and Inal.[13] Briefly, we mixed zinc oxide powder (ZnO, $\approx$100 μm, $>$99.5% purity) and boron powder in a molar ratio of 1:8, and pressed the mixture in a mold at room temperature and a pressure of 0.4 GPa to produce a pellet. The pellet was then sintered at a pressure of 0.18 GPa in Ar and 1800 °C for 4 h. Kayhan and Inal[13] proposed that crystalline B_6O is formed by the following reaction: $8B+ZnO \rightarrow B_6O+2B+Zn(g)\uparrow$, with the excessive boron to minimize undesirable oxidation due to the presence of residual oxygen and water in the sintering reactor. For the verification of the chemical composition and crystalline structure of our B_6O sample, we used a Philips X'PERT x-ray diffractometer (Cu K_α radiation, in θ–2θ mode).

B. XPS measurements of positions of Fermi level, valence-band maximum and core levels

All XPS data were obtained from a PHI Quantum 2000 XPS system, which has a monochromatic Al K_α source, a surface charge neutralizer, and a low-energy argon ion gun. Spectra were taken with a 45° polar angle of detection and calibrated to Au $4f_{7/2}$ at 84.0 eV from a sputter-cleaned gold foil.

During an XPS analysis, the Fermi levels (FLs) of the spectrometer and a metallic or semiconducting sample are considered to be aligned, with no energy difference detectable by XPS. The flow of photoemission current across the sample to the spectrometer ground, normally with a current density in the proximity of 10 pA/cm^2, will merely induce a surface potential less than 0.01 eV provided that the resistivity for a 1-mm-thick sample is not more than 10^{10} Ω cm. As a rule-of-thumb reference, undoped silicon has a resistivity of 2.3×10^5 Ω cm at room temperature. Hence, misalignment of FL between a sample and the spectrometer is negligible unless the sample is highly insulating or the photon source is extremely bright (like an intense synchrotron radiation beam). As such, the FL position of any unknown sample can be assumed to be the same as that of the gold reference sample constantly residing in the spectrometer. In this work, we collected the experimental valence-band (VB) spectrum of this gold sample, as shown by the summary schematic diagram in Fig. 2, with a spectrometer pass energy of 60 eV. The specification of spectrometer pass energy is very important because this fixed the spectrometer spectral resolution (i.e., the extent of spectral peak broadening) and thus the onset position of the VB photoemission. In the present case, the onset was located at -0.49 eV, with the zero point of the energy scale always calibrated by Au $4f_{7/4}$ at 84.0 eV. If one follows this same set of measuring conditions, one would expect the following results.

- Any metallic sample should give a photoemission onset at -0.49 eV.
- Any nonmetallic sample with negligible surface charging should have a photoemission onset located at a binding energy value higher than -0.49 eV, and the difference gives the separation between its valence-band maximum (VBM) and FL (referred as E_{FL} in this article). Indeed, this methodology has been used in studies of surface band bending and FL pinning of semiconductors.[2] Since every nonmetallic material can have, in principle, a variable E_{FL} at least from zero (FL reaching VBM) to its bandgap energy E_g (FL reaching its conduction-band minimum), all core-level binding energy data of this material in reference to its FL ($E_{b,FL}$) can also vary in the range of 0 to E_g. For example, we have reported[2c] $E_{b,FL}$ for Si $2p_{3/2}$ of silicon wafers with different doping conditions and surface state conditions in the range of 98.8 to 99.9 ± 0.1 eV. Clearly, a nonmetallic material can have a range of $E_{b,FL}$ values, and each value describes a combination of the chemical state and electronic state of the material. Hence, we advocate that XPS analysis of all nonmetallic samples should always follow this measurement methodology for the determination of E_{FL} and $E_{b,FL}$ in the same analysis. We estimate that if measurements are conducted carefully, the error of E_{FL} can be less than ±0.1 eV. Once E_{FL} is determined, binding energy data can also be reported by measuring them from VBM instead of from the FL. The value, $E_{b,VBM}$, is thus FL independent. For example, $E_{b,VBM}$ for Si $2p_{3/2}$ is always at 98.8 ± 0.1 eV, regardless of its doping nature.
- When a surface charging potential is experienced on a nonmetallic sample during XPS analysis, the surface charging potential can be determined by sputter depositing a gold overlayer of less than 1 nm on the sample. In such an analysis operation, the difference between the Au $4f_{7/4}$ of this gold overlayer and 84.0 eV gives the surface charging potential. Other research groups have used C $1s$ of graphitic carbon, which is a surface contaminant present on most samples, to determine surface charging potential. Typically, a reference value of 285.0 eV is adopted in this method. In addition to these two methods, silver deposition (Ag $3d_{5/2}$ at 368.2 eV) has also been used to replace gold with equal success. Although the error induced by surface charging can be eliminated by these or other valid methods,[1] the variable E_{FL} nature of all nonmetallic samples should still be addressed by the measurements of both E_{FL} and $E_{b,FL}$.

Finally we want to reiterate the following two technical notes relevant to the review of XPS methods for nonmetallic samples.

(a) It is important that the photoemission onset of the gold reference and the unknown sample should be measured with the same spectrometer pass energy. For example,

Downloaded 07 Apr 2011 to 158.132.161.9. Redistribution subject to AIP license or copyright; see http://jap.aip.org/about/rights_and_permissions

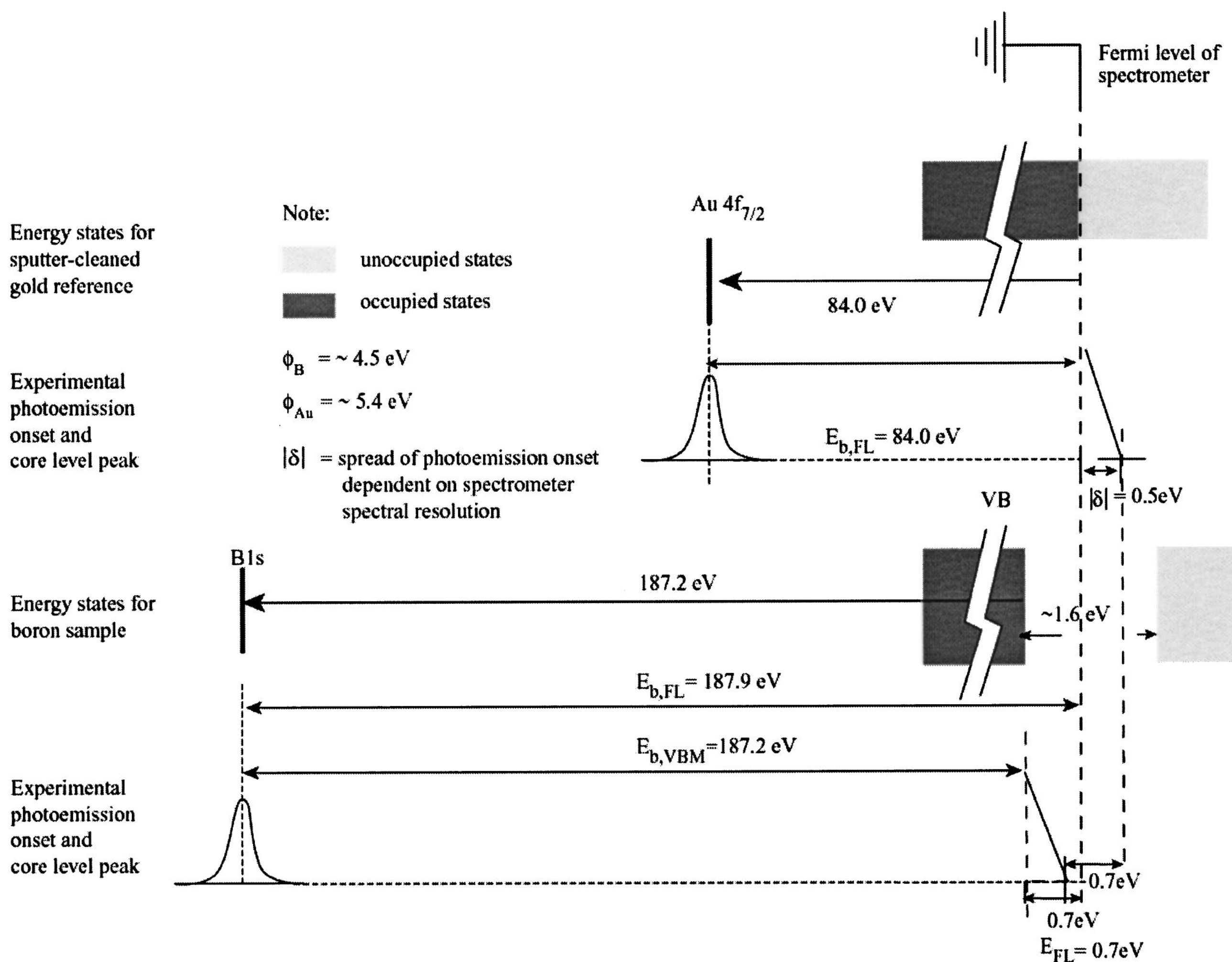

FIG. 2. Schematic diagram summarizing the conceptual energy bands and core levels of gold and β_r-B, together with their simplified XPS data.

for the same gold reference, its photoemission onset will move towards a higher binding energy when the pass energy is reduced because this gives a higher spectral resolution and smaller peak broadening. In comparison, the peak position of all core-level peaks should not be changed by a variation in pass energy because peak broadening does not affect the location of the peak centroid. In addition, we note that even if all FL alignment problems have been eliminated by the previously presented Au, Ag, or graphitic carbon referencing method, E_{FL} of the sample is not equal to the separation between the VBM photoemission onset and the zero point on the binding energy axis. This inequality arises from the inevitable spreading of the VBM edge due to the finite spectral resolution of the spectrometer. Once again, the most proper methodology requires the comparison of the VB photoemission onsets of the sample and a metal reference such as gold, which should be measured under the same pass energy, x-ray spot size, and other analysis conditions that affect spectral resolution.

(b) When surface charging and the effects of photon-beam irradiation on other measurement issues such as sample band bending are in doubt, measurements should be repeated by changing the photon beam intensity, for example, by a factor of 10. In the present work, no surface charging means no detectable changes with this tenfold reduction in x-ray intensity.

C. Neutralization of surface charges and other relevant measurement issues

When an electrically insulating sample is analyzed by XPS, a surface charge neutralizer is commonly used to minimize the degree of surface charging.[1] A typical surface charge neutralizer is a source of electrons with a variable kinetic energy of less than a few eV and a current density in the order of μA/cm^2. In principle, this source of electrons is adequate in overcompensating the loss of electrons from the sample surface due to photoemission and the low kinetic energy limits the charging potential arising from overcompensation. In our spectrometer, the neutralizer includes an additional source of low-energy positive argon ions to further enhance the uniformity of steady-state surface charging potential during XPS analysis. Once such a steady-state surface charging potential is established and maintained, the methods for measuring surface charging potential and E_{FL} can then be applied.

Downloaded 07 Apr 2011 to 158.132.161.9. Redistribution subject to AIP license or copyright; see http://jap.aip.org/about/rights_and_permissions

In reality, nonuniform samples may still impose problems and uncertainties in XPS measurements. Particularly, the component with the smallest E_{FL} will give VB photoemission, which makes the measurements of E_{FL} data of other components difficult. Special sample and analysis designs are required to address such practical issues. A series of measurements on samples containing individual constituents of the nonuniform subject is always desirable.

As a technical note, we add that for the analysis of a highly insulating sample, whether the sample is irradiated by x rays first or electrons from the neutralizer first, may make a difference. If the x-ray irradiation comes first, the positive surface potential due to photoemission may be high enough that this accelerates the neutralizing electrons and makes the secondary electron emission current density higher than the neutralizing electron current density. Surface charge neutralization will then fail.

III. RESULTS AND DISCUSSION ON BORON AND B_xO_y

A. Sputter-cleaned β_r-B

It is known that β_r-B is a semiconductor with a bandgap of ~1.6 eV. Hence, the XPS binding energy $E_{b,FL}$ of its B $1s$ core level depends on both its doping condition and surface band bending condition. With this in mind, one will not be surprised to see variable B $1s$ binding energy data in the literature,[9,10,15,16] even if all these data are corrected for surface charging during XPS analysis. In this work, we found that our polished and then sputter-cleaned β_r-B sample has a B $1s$ $E_{b,FL}$ at 187.9 eV, an E_{FL} of 0.7 eV, and no detectable surface charging as verified by spectral peak positions being independent to the intensity of x-ray irradiation. The data are shown in both Figs. 2 and 3. The results give an $E_{b,VBM}$ value of 187.2 eV, which can be used a good reference for all β_r-B.

The measured E_{FL} of 0.7 eV indicates that our boron sample has a FL slightly below its midgap. To independently check this finding, we applied the conventional Hall measurement method to the sample. We found that the majority carrier is indeed holes and the hole density is $10^{11}/cm^3$. Hence, the bulk FL is also slightly below midgap. As such, there is little surface band bending on our β_r-B sample.

In the context of our methodology and results, we estimate that in the surface science study of β_r-B (111) by Foo *et al.*,[16] the sample surface should have an E_{FL} at 0.5 eV, as they found an $E_{b,FL}$ of B $1s$ at 187.7 eV. Although no calibration was given in this study, we found from another XPS study of this research group[10] its calibration practice with Ag $3d_{5/2}$ at 368.3 eV. This calibration reference was similar to ours. Since they showed no data on the E_{FL} of the bulk of the sample, we cannot deduce if there was any surface band bending on the sample. In comparison, the $E_{b,FL}$ values of 187.2 and 187.3 eV previously reported by Moddeman *et al.*[9] and Lau *et al.*,[17] respectively, imply that these samples should have a surface FL quite close to VBM. On the other hand, the sample of Joyner *et al.*[15] would have a surface Fermi level slightly above the midgap, as an $E_{b,FL}$ of B $1s$ at 188.0 eV was measured and their calibration used Au $4f_{7/2}$ at 83.8 eV. Expressed in our calibration reference, the E_{FL} value of their sample should be 1.0 eV.

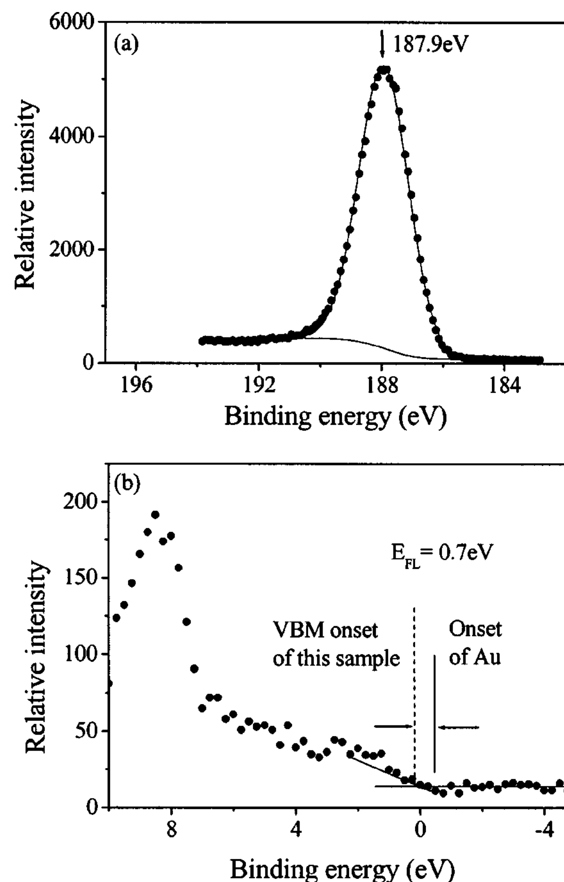

FIG. 3. XPS data of sputter-cleaned β_r-B: (a) B $1s$ spectrum; and (b) VB spectrum (no surface charging during analysis, and calibration with Au $4f_{7/2}$ at 84.0 eV).

To conclude this section on β_r-B, we cite the summary report on the locations of hole and electron energy states inside the bandgap of β_r-B published by Kimura.[5] The report and the relevant results cited therein suggest that β_r-B may have an acceptor band at about 0.2 eV above VBM and four donor bands at 0.8, 1.0, 1.2, and 1.4 eV above VBM. The presence of these gap states in different intensity combinations, together with a variation in the amounts of shallow dopant impurities, can explain all the β_r-B data in the present article. Admittedly, multiple combinations of these factors can give the same E_{FL} value, and other measurements are required to eliminate the irrelevant ones.

B. B_2O_3

Since B_2O_3 represents the fully oxidized form of boron, we measured $E_{b,FL}$ and $E_{b,VBM}$ of a polished B_2O_3 solid, which turned out to be 193.6 and 190.5 eV respectively. The former was determined by sputter-deposited 1 nm of gold on the sample. The measurement thus gives an E_{FL} of 3.1 eV. Li *et al.*[21] suggested that the theoretical bandgap of B_2O_3 is 6.2 eV. Hence, the surface FL of our B_2O_3 reference lies close to its midgap. This suggests that the absence of any fixed charge in our B_2O_3 reference. In comparison, Joyner *et al.*[18] reported an $E_{b,FL}$ of 193.4 eV for their B_2O_3 sample. After

Downloaded 07 Apr 2011 to 158.132.161.9. Redistribution subject to AIP license or copyright; see http://jap.aip.org/about/rights_and_permissions

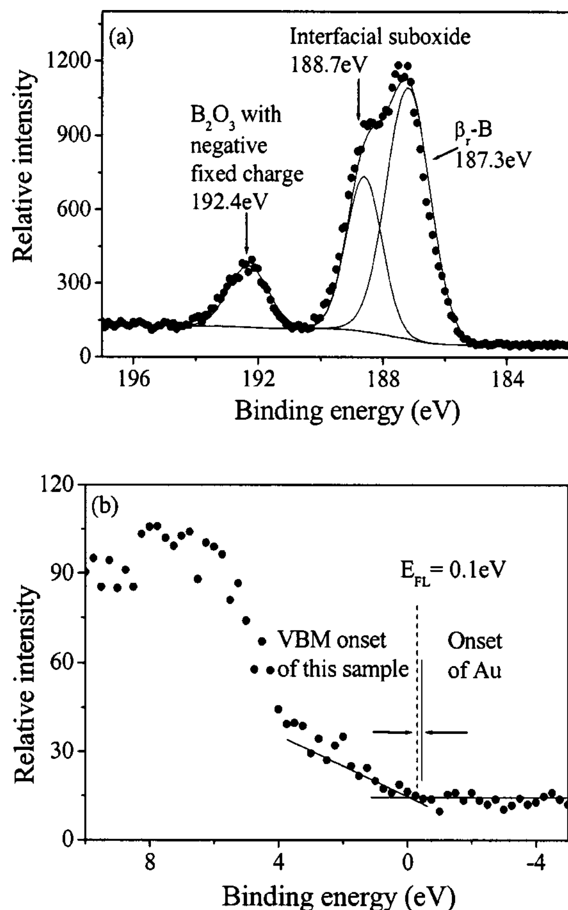

FIG. 4. XPS data of oxidized β_r-B surface: (a) B 1s spectrum and (b) VB spectrum.

corrections for the calibration difference, the $E_{b,\mathrm{FL}}$ of their B_2O_3 sample should also be at 193.6 eV. If we assume that our B_2O_3 has no fixed charge, an $E_{b,\mathrm{FL}}$ measurement lower than 193.6 eV would suggest the presence of negative fixed charge in the oxide. An example of this phenomenon can be found in the following section.

C. Surface oxidation of sputter-cleaned crystalline boron

In this work, we used a simple surface oxidation procedure to convert the sputter-cleaned boron sample to a typical dielectric-on-semiconductor system, in order to collect further information on the electronic structures of boron, boron suboxide, and boron oxide. The B 1s spectral data, as shown in Fig. 4(a), show the presence of mainly three chemical components in the analyzed region. The absence of surface charging was confirmed by the absence of any spectral peak shift for a tenfold reduction in the intensity of x-ray irradiation. The peak at 187.3 eV is attributed to elemental boron, and the other two peaks at higher binding energies are attributed to a boron suboxide and B_2O_3. A three-layer structure of B_2O_3/boron suboxide/boron was subsequently confirmed by angle-dependent XPS. With the assumption of this structure, we examined the boron and oxygen atomic concentration data as a function of analysis angles, and reached a structure model of $1.2\,\mathrm{nm}\,B_2O_3/2\,\mathrm{nm}\,B_xO_y$/B. The VB spectrum, as shown in Fig. 4(b), gives an E_{FL} of 0.1 eV. We thus infer that the β_r-B under the oxide structure has an upward band bending of 0.6 eV, most probably caused by the presence of negative fixed charge in the oxide structure. Indeed, the $E_{b,\mathrm{FL}}$ value of the B_2O_3 on this sample is 1.2 eV lower than that of the bulk B_2O_3 reference. This is consistent with our hypothesis of the presence of negative fixed charge in the oxide structure. In conclusion, our oxidation process induced the formation of an approximate structure of $2.0\,\mathrm{nm}\,B_2O_3/1.2\,\mathrm{nm}\,B_xO_y$/B. The bulk β_r-B has an E_{FL} value close to 0.7 eV, as measured prior to the surface oxidation. The negative charge trapped in the oxide overlayer induced an upward band bending, with a negative surface potential of 0.6 eV on β_r-B below the oxide and a potential drop of 0.6 eV across the oxide overlayer. The total surface potential on the oxide is thus 1.2 eV. The data also indicate that in the β_r-B below the oxide, its FL can move easily from $E_{\mathrm{FL}}=0.7$ to 0.1 eV with the trapped charge in the oxide. The absence of gap states in this band segment is consistent with the summary report by Kimura.[5]

In comparison, Foo *et al.*[15] found $E_{b,\mathrm{FL}}$ data for B 1s of β_r-B and B_2O_3 at 187.9 and 194.0 eV, respectively, when they evaporated a thin layer of B_2O_3 on β_r-B(111), which had an $E_{b,\mathrm{FL}}$ value of 187.7 eV prior to the oxide deposition. Assuming that their calibration was the same as ours, we infer that their oxide overlayer carried some positive fixed charge and this caused an increase of 0.4 eV in $E_{b,\mathrm{FL}}$ of B 1s for B_2O_3. In turn, this positive fixed charge in the oxide overlayer induced a downward band bending of the β_r-B below the oxide by 0.2 eV. In this case, the potential drop across the oxide (0.4 eV) can be more than that of the semiconductor (0.2 eV) because the presence of several donor bands above the midgap can effectively limit the FL movement from midgap to the conduction band. In fact, the donor bands at 0.8, 1.0, and 1.2 eV can be the limiting factors against the development of a semiconductor surface potential higher than 0.2 eV.

In another relevant study, Moddeman *et al.*[9] made a thorough angle-dependent analysis of surface oxide on boron (formed by heating at 400 °C for 24 h) and reported a three-layer structure of B_2O_3/B_3O/B. The stoichiometry of the middle layer is more boron rich than that in our surface oxide structure. Putting aside the differences between their oxidation conditions and ours, we view that both this and our own structure model are approximations of the real structures. The interface between suboxide and element boron is not atomically sharp in the lateral dimension of the XPS analysis (0.1 mm in diameter in our study), as indicated by both sets of angle-dependent data. Regarding surface potential across the oxide–semiconductor structure, we found it difficult to deduce much information from the data given by Moddeman *et al.*[9] because they shifted all raw spectra containing B_2O_3 by aligning them with a fixed B 1s peak for B_2O_3 at 192.4 eV. In our opinion, this referencing technique is not proper.

D. B_6O

The x-ray diffraction (XRD) pattern of our B_6O sample (Fig. 5) is almost identical to that of the sintered bulk B_6O

Downloaded 07 Apr 2011 to 158.132.161.9. Redistribution subject to AIP license or copyright; see http://jap.aip.org/about/rights_and_permissions

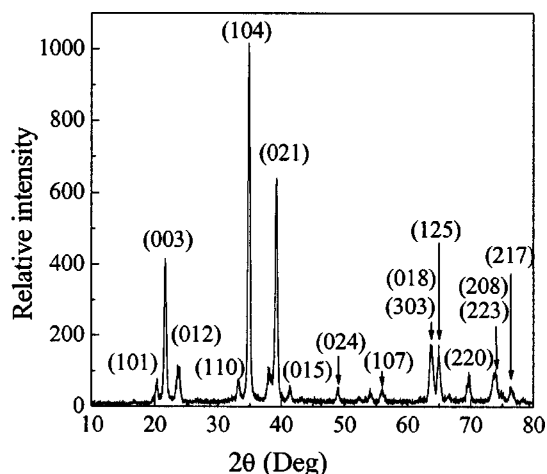

FIG. 5. XRD data for supporting the composition and phase purity of our B_6O sample.

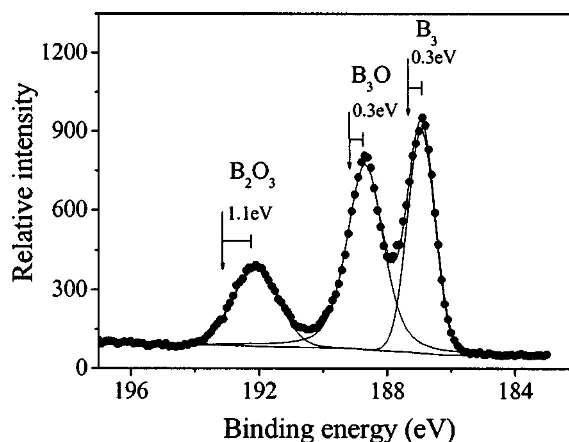

FIG. 6. B 1*s* spectrum of B_6O, showing effects of intentional negative surface charging (↓ denotes peak position prior to the application of negative surface charging).

prepared Rizzo *et al.*[8] The phase purity is also better than the sample prepared by Kayhan and Inal,[13] probably because we used a sintering condition of 180 MPa and 1800 °C to replace the original condition suggested by Kayhan and Inal (40 MPa and 1600 °C). These comparisons thus support the validity of our preparation of the superhard B_6O material. The raw XPS B 1*s* spectrum of our B_6O pellet sample has a spectral profile almost identical to those of Moddeman *et al.*[9] and Belyansky *et al.*[10] All three sets of data consistently show a very small peak in the spectral region for B_2O_3 and two almost equally strong peaks in the spectral region of pure boron and boron suboxide. In addition, in all three data sets, the energy difference between these two strong peaks is about 1.7–1.8 eV and each peak is very sharp (full width at half-maximum of about 1.5 eV). The similarities further support the validity of our analysis of B_6O.

With our methodology for nonmetallic materials, we found that the $E_{b,\mathrm{FL}}$ for B 1*s* of the three components are 187.1, 188.9, and 193.2 eV, with E_{FL} at 1.7 eV. In addition, we confirmed experimentally that the pellet showed no surface charging during XPS analysis. In the present work, we further found that sputter-etching of the sample caused a depletion of B_2O_3 and shrinking the energy difference between the two strong distinct peaks, together with peak broadening. Therefore, we postulate that B_2O_3 are a grain-boundary impurity, and we adopt the model of Moddenman *et al.*[9] that the two equally strong and distinct peaks represent the two groups of boron atoms in the unit cell of B_6O (Fig. 1); that is the six boron atoms with no oxygen neighbor (the B_3 group) and the six boron atoms with oxygen neighbor (the B_3O group). Although the semiconductor properties of B_6O have not yet been discussed much in the literature, previous theoretical data[11] and preliminary experimental data[12] both suggested a bandgap of about 2 eV. If this is accurate, our observed E_{FL} value of 1.7 eV would suggest that our B_6O sample had a relatively high electron carrier density. This is consistent with our observation that the sample was surprisingly electrically conductive.

Most interestingly, when we intentionally charged the surface negatively with electron flooding on our B_6O sample, we observed that while the B_3 group and B_3O group were shifted by the same amount of about 0.3 eV, the B_2O_3 peak was shifted by 1.1 eV, as shown in Fig. 6. Hence, electrons flooding the surface B_2O_3 overlayer of B_6O caused an upward band bending of the B_6O semiconductor by about 0.3 eV. Most probably the FL is either touching the conduction-band minimum of B_6O or is touching a donor band such that the negative surface potential across the oxide overlayer (0.8 eV) is much higher than across the depletion region of the semiconductor at the oxide–semiconductor interface.

In comparing our data and interpretations with those in the literature, we judge that although Moddeman *et al.*[9] hold the credit of reporting the first set of high-resolution XPS data on B_6O and making an insightful correlation of the XPS data to its bonding configuration consisting of the B_3 group and B_3O group, their incorrect messaging of the spectral data with a B_2O_3 reference at 192.4 eV causes a loss of some important data about their samples and this nonmetallic system. Belyansky *et al.*[10] subsequently reported the $E_{b,\mathrm{FL}}$ data on the B 1*s* core levels of the boron components, with silver as their FL reference and a calibration 0.1 eV higher than ours. They reported that the data for the B_3 group and B_3O group are 187.4 and 189.2 eV, respectively, and we read from their spectrum a value of 193.2 eV for the B_2O_3 component. Therefore, we infer that there is little fixed charge in the oxide overlayer on their sample, and the E_{FL} of the B_6O semiconductor is 1.4 eV, 0.3 eV lower than that of our sample. This suggests that their sample is purer than ours.

V. CONCLUSIONS

Our studies on β_r-B, B_2O_3, surface oxidation of β_r-B, and B_6O illustrate that not unlike all other materials, an XPS peak shift can be caused by a change in chemical state and bonding configuration. The shifts of B 1*s* peaks for β_r-B versus B_2O_3 and for the B_3 group versus the B_3O group in B_6O provide some good evidence to substantiate this conventional wisdom of XPS. In addition, an XPS shift in nonmetallic materials can also be caused by a change in occupancy of electronic states of impurities and charge trapping defects, even for an impurity/defect concentration in the part-

Downloaded 07 Apr 2011 to 158.132.161.9. Redistribution subject to AIP license or copyright; see http://jap.aip.org/about/rights_and_permissions

per-million level. In the present work, we have applied this concept to enrich our XPS studies of boron and B_xO_y, and indeed found an intriguing variety of surface and interfacial physical conditions of β_r-B and B_6O and different charge trapping conditions for B_2O_3. We view that all future XPS analysis of nonmetallic materials should follow a methodology similar to that in this work, to obtain information on both the chemical and electrical nature of the materials.

ACKNOWLEDGMENTS

The work described in this article was supported by the Research Grant Council of the Hong Kong Special Administrative Region (Project Code: PolyU 5186/99P, with account code B-Q281, and Project Code: CUHK 4440/99E).

[1] For a comprehensive review of XPS, see, e.g., *Practical Surface Analysis*, 2nd ed., edited by D. Briggs and M. P. Seah (Wiley, Chichester, 1990).
[2] For discussion of XPS that specifically addresses FL referencing, see, e.g., (a) E. A. Kraut, R. W. Grant, and S. P. Kowalczyk, Phys. Rev. B **28**, 1965 (1983); (b) T. L. Barr, Crit. Rev. Anal. Chem. **22**, 115 (1991); (c) W. M. Lau and X.-W. Xu, Surf. Sci. **245**, 345 (1991); (d) L. J. Huang and W. M. Lau, Appl. Phys. Lett. **60**, 1108 (1992); (e) Q. Zhao, Z. W. Deng, R. W. M. Kwok, and W. M. Lau, J. Vac. Sci. Technol. A **18**, 2271 (2000).
[3] For background information on boron and its compounds, see, e.g., *Boron and Refractory Borides*, edited by V. I. Mathovich (Springer, Berlin, 1977).
[4] For an overview of bonding configurations and crystal structures including those of boron, see, e.g., J. Donohue, *The Structures of the Elements* (Wiley, New York, 1974).
[5] K. Kimura, Mater. Sci. Eng., B **19**, 67 (1993), and references cited therein.
[6] Several reviews have been published on boron-rich compounds, e.g., D. Emin, Phys. Today **40**, 55 (1987); T. Lundström and Y. G. Andreev, Mater. Sci. Eng., A **209**, 16 (1996).
[7] A. R. Badzian, Appl. Phys. Lett. **53**, 2495 (1988).
[8] H. F. Rizzo, W. C. Simmons, and H. O. Bielstein, J. Electrochem. Soc. **109**, 1079 (1962).
[9] W. E. Moddeman, A. R. Burke, W. C. Bowling, and D. S. Foose, Surf. Interface Anal. **14**, 224 (1989).
[10] M. Belyansky, M. Trenary, and C. Ellision, Surf. Sci. Spectra **3**, 147 (1995), and references cited therein.
[11] S. Lee, D. Kim, D. M. Bylander, and L. Kleinman, Phys. Rev. B **44**, 3550 (1991).
[12] H. Hubert, B. Devouard, L. A. J. Garvie, M. O'Keeffe, P. R. Buseck, W. T. Petuskey, and P. McMillan, Nature (London) **391**, 376 (1998).
[13] I. O. Kayhan and O. T. Inal, J. Mater. Sci. **34**, 4105 (1999); Mat. Tech & Adv. Per. Mat. **15**, 12 (2000).
[14] D. He, Y. Zhao, L. Daemen, J. Qian, T. D. Shen, and T. W. Zerda, Appl. Phys. Lett. **81**, 643 (2002).
[15] D. J. Joyner, O. Johnson, and D. M. Hercules, J. Am. Chem. Soc. **102**, 1910 (1980).
[16] W. C. Foo, J. S. Ozcomert, and M. Trenary, Surf. Sci. **255**, 245 (1991).
[17] W. M. Lau, R. Yang, B. Y. Tong, and S. K. Wong, Mater. Res. Soc. Symp. Proc. **105**, 163 (1988).
[18] D. J. Joyner and D. M. Hercules, J. Chem. Phys. **72**, 1095 (1980).
[19] X. Y. Liu, X. D. Zhao, W. M. Hou, and W. H. Su, J. Alloys Compd. **223**, L7 (1995).
[20] For research results on boron suboxide films, see, e.g., C. Doughty, S. M. Gorbatkin, T. Y. Tsui, G. M. Pharr, and D. L. Medlin, J. Vac. Sci. Technol. A **15**, 2623 (1997); D. Music, J. M. Schneider, V. Kugler, S. Nakao, P. Jin, M. Östblom, L. Hultman, and U. Helmersson, *ibid.* **20**, 335 (2002); H. Huang, C. W. Ong, B. Zheng, R. W. M. Kwok, W. M. Lau, and J. W. He, (in press).
[21] D. Li and W. Y. Ching, Phys. Rev. B **54**, 13616 (1996).

Downloaded 07 Apr 2011 to 158.132.161.9. Redistribution subject to AIP license or copyright; see http://jap.aip.org/about/rights_and_permissions